Effect of Varying the Transition State Geometry on N + N_2 Vibrational Deexcitation Rate Coefficients

E. Garcia

Departamento de Quimica Fisica, Universidad del Pais Vasco, Vitoria, Spain

A. Laganà*

Dipartimento di Chimica, Università di Perugia, Perugia, Italy

Received: January 30, 1997; In Final Form: April 18, 1997[⊗]

The dependence of the transition state on the vibrational deexcitation in the N + N_2 reaction has been investigated by using different largest angle generalized rotating bond order (LAGROBO) model potentials. Using the LAGROBO functional representation of the interaction, it has been possible to vary both the angle and bond length values at the saddle for reaction. Quasiclassical and quantum infinite order sudden values of detailed cross sections and rate coefficients calculated on these modified surfaces for the N + N_2 reaction indicate that relative efficiencies of processes occurring in N_2 nonequilibrium systems (*e.g.* plasmas) are rather sensitive to the geometrical characteristics of the transition state.

1. Introduction

The deexcitation of vibrationally excited nitrogen molecules by nitrogen atoms is thought to be important in modeling the complex mechanism in nitrogen plasmas under electrical discharges[1] as well as in modeling processes taking place around reentering spacecrafts.[2,3]

Extended dynamical calculations of state to state cross sections and rate coefficients of the N + N_2 reaction were performed in the past using a potential energy surface (PES) of the LEPS type having a collinear transition state geometry.[4,5] These calculations showed that the efficiency of state to state processes is sensitive to both initial vibrational energy and the difference between initial and final state.

Recent theoretical studies[6,7] casted some doubts on the collinearity of the transition state of this reaction. This has suggested a sensitivity analysis of state to state reactive properties to the transition state geometry.

Unfortunately, LEPS PESs (as other usual functional representations of the interaction) are difficult to modify locally by playing with the values of the parameters. On the contrary, the modification of the height of the barrier, of its location, and of the shape of the window to reaction is easy when using a recently proposed functional representation of the PES (LAGROBO).[8,9]

The LAGROBO formulation of the PES was obtained by generalizing the definition of the rotating bond order (ROBO) model[10,11] to the description of the potential energy surface (PES) of systems with more than one channel open to reaction. The ROBO model potential was designed to describe the interaction relative to the process of transferring the intermediate atom (*e.g.* the I atom in the K + IJ → KI + J process). It is formulated as

$$V_I^{ROBO}(m_I,\alpha_I,\Phi_I) = D_I(\alpha_I,\Phi_I)\, F_I(m_I;\alpha_I,\Phi_I) \qquad (1)$$

where D_I and F_I are functions of the m_I and α_I ROBO coordinates. At a given value of the included angle Φ_I ($\Phi_I \equiv \widehat{KIJ}$) formed by the r_{KI} and r_{IJ} internuclear distances, these coordinates are defined in terms of the bond order variables n_{KI} and n_{IJ} ($n_{LM} = \exp[-\beta_{LM}(r_{LM} - r_{eLM})]$, with r_{eLM} and β_{LM} being respectively the equilibrium distance and a parameter related to the force constants of the LM diatom) by the relationships

$$m_I = \sqrt{n_{KI}^2 + n_{IJ}^2} \qquad (2)$$

$$\tan \alpha_I = n_{IJ}/n_{KI}$$

The LAGROBO generalization consists of formulating the global potential as a weighted sum of the ROBO potentials of the different processes and of assigning the highest weight to the process occurring with the largest included angle. Therefore, for the A + BC atom−diatom system reacting to give either AB + C or AC + B, the LAGROBO potential is formulated as

$$V^{LAGROBO}(r_{AB},r_{BC},r_{AC}) = \sum_I^{A,B,C} w_I(\Phi_I)\, V_I^{ROBO}(m_I,\alpha_I,\Phi_I) \qquad (3)$$

where the weighting coefficient w_I is defined as

$$w_I(\Phi_I) = \frac{g_I(\Phi_I)}{\sum_J^{A,B,C} g_J(\Phi_J)} \qquad (4)$$

with $g_I(\Phi_I)$ being a damping function of the type

$$g_I(\Phi_I) = \frac{1}{2}\,(1 + \tanh[\gamma_I(\Phi_I - \Phi_I^\circ)]) \qquad (5)$$

When the included angle Φ_I deviates from Φ_I°, $g_I(\Phi_I)$ tends to 1 as Φ_I goes to 180°, while it tends to 0 as Φ_I goes to 0°. The value of γ_I determines the speed of variation of the function.

The LAGROBO potential has been already applied to the fitting of *ab initio* and empirical potential energy values of the H + H_2 and N + N_2 symmetric reactions.[8] It was also used to construct the PES of the O(^{1} D) + HCl reaction.[9]

In this paper, the comparison of reactive properties of PESs having different transition state geometries is performed. To this end, the ability of the LAGROBO model to generate potential energy surfaces having the desired local features is discussed in the second section. In section 3, the values of

[⊗] Abstract published in *Advance ACS Abstracts,* June 1, 1997.

S1089-5639(97)00377-0 CCC: $14.00

TABLE 1: Coefficients of the LAGROBO Surface[a]

	L0	L1	L2	L3
Φ_{I1}^{TS}	180°	120°	120°	125°
Φ_{I2}^{TS}	180°	180°	180°	180°
c_{I11}	35.69	35.69	35.69	32.28
c_{I12}	6.60	43.99	43.99	53.03
c_{I13}	−0.61	42.13	42.13	24.49
c_{I14}	1.47	37.38	37.38	24.73
c_{I21}	−0.0367	−0.0367	−0.0367	−0.0367
c_{I22}	−0.0318	−0.0318	−0.0318	−0.0318
c_{I23}	0.0064	0.0064	0.0064	0.0064
c_{I24}	−0.0059	−0.0059	−0.0059	−0.0059
γ_I	50	50	10	50
Φ_I°	75°	75°	75°	75°

[a] c_{I1k} in kcal/mol.

detailed cross sections and vibrational deexcitation rate coefficients calculated on different LAGROBO surfaces using both quasiclassical (QCT)[12] and quantum reactive infinite order sudden (RIOS)[13] techniques are analyzed.

2. The LAGROBO Surfaces

A first test of the flexibility of the LAGROBO model[8] in describing the interaction of the N + N_2 system was carried out by fitting the existing LEPS. To illustrate the fitting procedure, we give in the following a brief description of the parameters of the used LAGROBO model.

Since the asymptotic limits of the LEPS are Morse potentials, the three ROBO potentials were given the form (for sake of generality the process index I is not dropped from the notation even if the three atoms are identical)

$$V_I^{ROBO}(m_I,\alpha_I,\Phi_I)\, D_I(\alpha_I,\Phi_I)\left[\frac{m_I^2}{a_I^2(\alpha_I,\Phi_I)} - 2\frac{m_I}{a_I(\alpha_I,\Phi_I)}\right] \quad (6)$$

The D_I and a_I coefficients indicate, respectively, the depth and location in m_I of the fixed Φ_I energy minimum of the reaction channel as α_I varies from the reactant to product asymptote. Accordingly, the values of D_I and a_I at the asymptotes (α_I = 0° and 90°, respectively) were chosen to reproduce the dissociation energy D_{eNN}, the equilibrium distance r_{eNN}, and the exponential factor β_{NN} of the N_2 Morse diatomic potential (D_{eNN} = 228.40 kcal/mol, r_{eNN} = 1.0977 Å, and β_{NN} = 2.689 Å^{-1}).[14] In order to keep the formulation of the ROBO potential as simple as possible, D_I and a_I coefficients were given the following dependence on α_I:

$$D_I(\alpha_I,\Phi_I) = D_{eNN} - b_{I1}(\Phi_I)\sin(2\alpha_I) \quad (7)$$

$$a_I(\alpha_I,\Phi_I) = 1 + b_{I2}(\Phi_I)\sin(2\alpha_I) \quad (8)$$

and b_{Ij} coefficients were given the following polynomial dependence on Φ_I:

$$b_{Ij} = \sum_{k=1}^{k_{max}} c_{Ijk}(\Phi_{Ij}^{TS} - \Phi_I)^\zeta \quad (9)$$

For the LAGROBO potential (L0) obtained by fitting the existing LEPS, Φ_{Ij}^{TS} is 180°, ζ is 2(k − 1) and k_{max} is 4. As a result, one has a total of 8 c_{Ijk} coefficients. For the damping functions of eq 5 Φ_I° is 75° and γ_I is 50. The values of all the parameters of the L0 surface are given in the first column of Table 1.

A preliminary comparison of the features of the L0 model potential with those of the original LEPS was already made in ref 8. Heights and locations of the fixed Φ_N barriers to reaction for the different PESs are given in Tables 2 and 3 (column 1 for LEPS, column 2 for L0). As clearly indicated by the tables, both the height and the geometry of L0 well reproduce those of the LEPS. The most significant difference is the slope of the minimum energy path (MEP) of L0, which is larger than that of the MEP of the LEPS (that is, the MEP of L0 lies always slightly above that of the LEPS).

TABLE 2: Saddle Height[a]

Φ_N	LEPS	L0	L1	L2	L3
180°	35.7	35.7	80.5	80.5	80.5
150°	37.2	37.5	44.5	44.5	41.2
125°	42.3	42.4	36.0	36.0	32.3
120°	44.2	44.1	35.7	35.7	32.7
90°	70.5	70.4	56.6	56.6	61.1
60°	177.4	177.3	177.3	177.3	177.3

[a] In kcal/mol.

TABLE 3: Internuclear N−N Distance[a] at the Saddle

Φ_N	LEPS	L0	L1	L2	L3
180°	1.240	1.240	1.240	1.240	1.240
150°	1.243	1.244	1.244	1.244	1.244
125°	1.251	1.252	1.252	1.252	1.252
120°	1.254	1.254	1.254	1.254	1.254
90°	1.294	1.293	1.293	1.277	1.293
60°	1.530	1.522	1.522	1.324	1.522

[a] In Å.

To modify the height and the location of the transition state of the other LAGROBO PESs, we played with the analytic formulation of the b_{Ij} coefficients of eq 9 and with the value of the related c_{Ijk}, Φ_{I1}^{TS}, and γ_I parameters. In this way, we generated L1, L2, and L3, three new LAGROBO potential energy surfaces. For all these LAGROBO potentials, the ζ of eq 9 was set equal to k − 1 for b_{I1} and equal to 2(k − 1) for b_{I2} (except for that of L2, for which the value k − 1 was taken). At the same time, Φ_{I1}^{TS} was set equal to 120° for L1 and L2 and equal to 125° for L3 (it was equal to 180° for L0). The value of Φ_{I2}^{TS} was always set equal to 180°. To allow L1 and L2 to have the same height of the transition state as the LEPS, c_{I11} was set equal to that of L0. On the contrary, the value of c_{I11} of L3 was chosen so as to make the height of the transition state better agree with the indications of *ab initio* calculations.[7] Remaining c_{I1k} coefficients of L1, L2, and L3 were chosen to reproduce in Φ_N = 60°, the width of the collinearly centered window to reaction of the LEPS. A collinear barrier of 80 kcal/mol was enforced on L1, L2, and L3. For the damping function $g_I(\Phi_I)$, the value of γ_I was set equal to 50 (with the exception of L2 for which it was set equal to 10) and the value of Φ_I° equal to 75°.

The values of the parameters of the L1, L2, and L3 surfaces are given in the third, fourth, and fifth columns of Table 1, respectively. The characteristics (height and bond lengths) of the resulting fixed Φ_N barriers to reaction are given in the corresponding columns of Tables 2 and 3. The L1, L2, and L3 PESs have a bent transition state. The geometry of the transition state is the key difference between L0 and L1. In fact, while the height of the transition state is the same (35.7 kcal/mol) for both surfaces, the geometry of the L0 transition state is collinear, as is that of the LEPS. At the same time, the transition state of L3 differs in that it is high, 32.7 kcal/mol, and located at Φ_N 125°. The L1 and L2 surfaces have exactly the same dependence on the fixed angle barrier to reaction of Φ_N, while they differ in its location: L2 barriers always occur at internuclear distances smaller than those of L1, although such a difference is really significant only for strongly bent geometries.

TABLE 4: QCT $k_v(T)$ Rate Coefficients[a]

v	LEPS	L0	L1	L2	L3
			$T = 500$ K		
10	0.522(−15)	0.000(−00)	0.780(−15)	0.000(−00)	0.597(−14)
15	0.412(−13)	0.241(−13)	0.581(−13)	0.553(−13)	0.187(−12)
20	0.478(−12)	0.226(−12)	0.734(−12)	0.640(−12)	0.149(−11)
25	0.252(−11)	0.120(−11)	0.362(−11)	0.315(−11)	0.582(−11)
30	0.922(−11)	0.435(−11)	0.117(−10)	0.997(−11)	0.154(−10)
35	0.241(−10)	0.124(−10)	0.279(−10)	0.239(−10)	0.330(−10)
40	0.519(−10)	0.301(−10)	0.570(−10)	0.488(−10)	0.621(−10)
45	0.981(−10)	0.625(−10)	0.101(−09)	0.875(−10)	0.104(−09)
			$T = 1000$ K		
10	0.180(−12)	0.138(−12)	0.289(−12)	0.270(−12)	0.624(−12)
15	0.172(−11)	0.128(−11)	0.266(−11)	0.250(−11)	0.445(−11)
20	0.761(−11)	0.504(−11)	0.103(−10)	0.946(−11)	0.144(−10)
25	0.210(−10)	0.137(−10)	0.263(−10)	0.236(−10)	0.319(−10)
30	0.453(−10)	0.297(−10)	0.526(−10)	0.467(−10)	0.588(−10)
35	0.845(−10)	0.567(−10)	0.917(−10)	0.804(−10)	0.968(−10)
40	0.138(−09)	0.992(−10)	0.144(−09)	0.128(−09)	0.146(−09)
45	0.212(−09)	0.164(−09)	0.214(−09)	0.192(−09)	0.215(−09)
			$T = 2000$ K		
10	0.459(−11)	0.395(−11)	0.657(−11)	0.629(−11)	0.942(−11)
15	0.170(−10)	0.142(−10)	0.230(−10)	0.217(−10)	0.290(−10)
20	0.410(−10)	0.329(−10)	0.514(−10)	0.475(−10)	0.584(−10)
25	0.788(−10)	0.611(−10)	0.916(−10)	0.836(−10)	0.984(−10)
30	0.130(−09)	0.102(−09)	0.144(−09)	0.130(−09)	0.148(−09)
35	0.197(−09)	0.157(−09)	0.207(−09)	0.191(−09)	0.209(−09)
40	0.278(−09)	0.232(−09)	0.283(−09)	0.261(−09)	0.284(−09)
45	0.378(−09)	0.331(−09)	0.376(−09)	0.349(−09)	0.373(−09)
			$T = 4000$ K		
10	0.328(−10)	0.300(−10)	0.421(−10)	0.406(−10)	0.486(−10)
15	0.717(−10)	0.641(−10)	0.890(−10)	0.842(−10)	0.963(−10)
20	0.129(−09)	0.110(−09)	0.148(−09)	0.140(−09)	0.153(−09)
25	0.200(−09)	0.170(−09)	0.216(−09)	0.202(−09)	0.218(−09)
30	0.278(−09)	0.242(−09)	0.294(−09)	0.274(−09)	0.293(−09)
35	0.372(−09)	0.331(−09)	0.380(−09)	0.357(−09)	0.378(−09)
40	0.471(−09)	0.429(−09)	0.474(−09)	0.451(−09)	0.472(−09)
45	0.555(−09)	0.524(−09)	0.557(−09)	0.532(−09)	0.557(−09)

[a] In cm^3 $molecule^{-1}$ s^{-1}. $a(-b)$ reads as $a \times 10^{-b}$.

TABLE 5: RIOS $k_v(T)$ Rate Coefficients[a]

v	LEPS	L0	L1	L2	L3
			$T = 500$ K		
5	0.258(−18)	0.280(−18)	0.136(−18)	0.135(−18)	0.243(−17)
10	0.608(−15)	0.448(−15)	0.792(−15)	0.765(−15)	0.476(−14)
15	0.340(−13)	0.189(−13)	0.534(−13)	0.492(−13)	0.173(−12)
20	0.480(−12)	0.190(−12)	0.657(−12)	0.588(−12)	0.124(−11)
25	0.244(−11)	0.910(−12)	0.304(−11)	0.264(−11)	0.507(−11)
30	0.615(−11)	0.347(−11)	0.696(−11)	0.618(−11)	0.950(−11)
35	0.179(−10)	0.109(−10)	0.190(−10)	0.168(−10)	0.204(−10)
40	0.287(−10)	0.187(−10)	0.289(−10)	0.254(−10)	0.297(−10)
			$T = 1000$ K		
5	0.255(−14)	0.253(−14)	0.256(−14)	0.255(−14)	0.107(−13)
10	0.162(−12)	0.136(−12)	0.222(−12)	0.217(−12)	0.536(−12)
15	0.152(−11)	0.112(−11)	0.214(−11)	0.204(−11)	0.378(−11)
20	0.654(−11)	0.420(−11)	0.832(−11)	0.769(−11)	0.116(−10)
25	0.172(−10)	0.108(−10)	0.201(−10)	0.182(−10)	0.253(−10)
30	0.338(−10)	0.235(−10)	0.370(−10)	0.338(−10)	0.411(−10)
35	0.630(−10)	0.448(−10)	0.661(−10)	0.594(−10)	0.679(−10)
40	0.874(−10)	0.667(−10)	0.881(−10)	0.787(−10)	0.877(−10)
			$T = 2000$ K		
5	0.404(−12)	0.390(−12)	0.491(−12)	0.479(−12)	0.947(−12)
10	0.388(−11)	0.350(−11)	0.508(−11)	0.500(−11)	0.761(−11)
15	0.140(−10)	0.118(−10)	0.179(−10)	0.173(−10)	0.230(−10)
20	0.331(−10)	0.262(−10)	0.393(−10)	0.370(−10)	0.451(−10)
25	0.605(−10)	0.473(−10)	0.677(−10)	0.628(−10)	0.733(−10)
30	0.959(−10)	0.766(−10)	0.102(−09)	0.943(−10)	0.105(−09)
35	0.142(−09)	0.115(−09)	0.146(−09)	0.133(−09)	0.146(−09)
			$T = 4000$ K		
5	0.732(−11)	0.711(−11)	0.903(−11)	0.873(−11)	0.119(−10)
10	0.259(−10)	0.243(−10)	0.315(−10)	0.310(−10)	0.372(−10)
15	0.561(−10)	0.505(−10)	0.657(−10)	0.636(−10)	0.721(−10)
20	0.959(−10)	0.839(−10)	0.107(−09)	0.102(−09)	0.112(−09)
25	0.143(−09)	0.124(−09)	0.153(−09)	0.144(−09)	0.156(−09)

[a] In cm^3 $molecule^{-1}$ s^{-1}. $a(-b)$ reads as $a \times 10^{-b}$.

3. Dynamical Properties of LAGROBO PESs

3.1. The Calculations. To compare the reactive efficiencies of the four PESs, both QCT and quantum RIOS calculations were performed. Quasiclassical trajectory calculations were carried out by systematically varying both the initial vibrational number and the temperature. Considered initial vibrational numbers were $v = 10$, 15, 20, 25, 30, 35, 40, and 45. Considered temperature values were $T = 500$, 1000, 2000, and 4000 K. Calculations performed on the LEPS using different values for rotational and translational temperatures showed that the effect of varying the rotational temperature is not dramatic.[5,15] For this reason, here, the two temperatures were given the same value.

RIOS calculations were also performed for the same range of parameters and using the same computational procedures adopted for the LEPS.[15] The investigated range of energy extends up to 200 kcal/mol in steps of about 2 kcal/mol. The values of Φ_N considered for the angular integration are regularly spaced in cos Φ_N using a step of 0.0625. To mimic the effect of varying the initial rotational temperature, a j -shifting approximation was used. This means that the $\sigma_{vj,v'}(E_{tr})$ cross section summed over product rotational states for a given value of j was set equal to the value of the cross section for the ground rotational energy $\sigma_{v0,v'}(E^j_{tr})$ calculated at a value of the collision energy E^j_{tr} defined as $E^j_{tr} = E_{tr} - \epsilon^v_j$, with ϵ^v_j being the energy of the jth rotational state of the $v + 1$th vibrational level.

3.2. Thermal Rate Coefficients. A first indication of the kinetic and dynamic relevance of the different features of the used PESs can be obtained from a comparison of the values of thermal rate coefficient calculated for them. For all surfaces no appreciable reactivity was calculated at $T = 1000$ K as found by the experiment.[16] At $T = 3400$ K, the thermal rate coefficients calculated on the LEPS, L0, L1, L2, and L3 using the QCT method are, respectively, 7.1×10^{-13}, 7.0×10^{-13}, 10.4×10^{-13}, 10.4×10^{-13}, and 14.8×10^{-13} cm^3 $molecule^{-1}$ s^{-1}. These values agree reasonably well with the experiment (5×10^{-13} cm^3 $molecule^{-1}$ s^{-1}).[17] The agreement was found to be even more satisfactory when using the RIOS method. Values of the thermal rate coefficient calculated on the LEPS, L0, L1, L2, and L3 are 5.6×10^{-13}, 5.4×10^{-13}, 7.7×10^{-13}, 7.5×10^{-13}, and 11.3×10^{-13} cm^3 $molecule^{-1}$ s^{-1}, respectively. The values calculated using the j-shifting approximation (3.0×10^{-13}, 3.0×10^{-13}, 4.2×10^{-13}, 4.1×10^{-13}, and 6.2×10^{-13} cm^3 $molecule^{-1}$ s^{-1} on the LEPS, L0, L1, L2, and L3) also lead to a sufficiently good agreement with experiment. These results, though differing in more detailed properties, show that all these surfaces properly describe the overall reactive efficiency of the system. The main difference is that PESs having a bent transition state lead to more reactivity than those with a collinear transition state with a maximum effect for L3, which has a smaller barrier to reaction. On the contrary, the value of the internuclear distances at the transition state does not seem to affect significantly the reactivity of the system.

3.3. State Specific Reactivity. As already mentioned, a more detailed comparison of the dynamical and kinetic properties of the different PESs can be carried out by considering state specific ($k_v(T)$) rate coefficients calculated by starting from a given initial vibrational state of the reactants. Values of $k_v(T)$ calculated using QCT, pure RIOS, and j-shifting RIOS results are shown in Tables 4, 5, and 6 for reactants thermalized at $T = 500$, 1000, 2000, and 4000 K and v ranging from 5 to 45 in steps of 5. Since, as we shall comment more extensively in

TABLE 6: *j*-Shifting RIOS $k_v(T)$ Rate Coefficients[a]

v	LEPS	L0	L1	L2	L3
			$T = 500$ K		
5	0.132(−18)	0.144(−18)	0.699(−19)	0.691(−19)	0.124(−17)
10	0.317(−15)	0.233(−15)	0.413(−15)	0.399(−15)	0.249(−14)
15	0.180(−13)	0.100(−13)	0.284(−13)	0.261(−13)	0.926(−13)
20	0.260(−12)	0.102(−12)	0.357(−12)	0.319(−12)	0.677(−12)
25	0.135(−11)	0.494(−12)	0.169(−11)	0.147(−11)	0.285(−11)
30	0.344(−11)	0.191(−11)	0.390(−11)	0.345(−11)	0.543(−11)
35	0.101(−10)	0.619(−11)	0.108(−10)	0.960(−11)	0.116(−10)
40	0.168(−10)	0.108(−10)	0.169(−10)	0.148(−10)	0.174(−10)
			$T = 1000$ K		
5	0.133(−14)	0.132(−14)	0.133(−14)	0.133(−14)	0.564(−14)
10	0.864(−13)	0.726(−13)	0.118(−12)	0.116(−12)	0.289(−12)
15	0.832(−12)	0.612(−12)	0.117(−11)	0.111(−11)	0.210(−11)
20	0.368(−11)	0.233(−11)	0.469(−11)	0.434(−11)	0.660(−11)
25	0.992(−11)	0.614(−11)	0.116(−10)	0.105(−10)	0.149(−10)
30	0.198(−10)	0.136(−10)	0.217(−10)	0.198(−10)	0.245(−10)
35	0.381(−10)	0.267(−10)	0.400(−10)	0.359(−10)	0.412(−10)
40	0.503(−10)	0.380(−10)	0.512(−10)	0.456(−10)	0.510(−10)
			$T = 2000$ K		
5	0.217(−12)	0.209(−12)	0.263(−12)	0.257(−12)	0.513(−12)
10	0.215(−11)	0.193(−11)	0.282(−11)	0.278(−11)	0.428(−11)
15	0.802(−11)	0.670(−11)	0.103(−10)	0.990(−11)	0.133(−10)
20	0.194(−10)	0.152(−10)	0.232(−10)	0.218(−10)	0.270(−10)
25	0.366(−10)	0.281(−10)	0.411(−10)	0.381(−10)	0.452(−10)
30	0.593(−10)	0.466(−10)	0.633(−10)	0.584(−10)	0.658(−10)
35	0.819(−10)	0.652(−10)	0.856(−10)	0.778(−10)	0.857(−10)
			$T = 4000$ K		
5	0.408(−11)	0.397(−11)	0.504(−11)	0.487(−11)	0.670(−11)
10	0.150(−10)	0.140(−10)	0.183(−10)	0.180(−10)	0.219(−10)
15	0.335(−10)	0.300(−10)	0.396(−10)	0.383(−10)	0.441(−10)
20	0.591(−10)	0.512(−10)	0.664(−10)	0.633(−10)	0.703(−10)
25	0.874(−10)	0.747(−10)	0.945(−10)	0.888(−10)	0.973(−10)

[a] In cm^3 $molecule^{-1}$ s^{-1}. $a(-b)$ reads as $a \times 10^{-b}$.

the next subsection, RIOS rate coefficients are directly derived from state (v) to state (v') fixed energy cross sections by integrating over translational energy, at high initial vibrational numbers the range of considered total energy values is not large enough to ensure that the integration interval is fully covered. This is not the case with QCT calculations, for which rate coefficients are calculated by using a proper sampling of initial conditions.

For all PESs, and for both QCT and RIOS methods, $k_v(T)$ increases with the temperature more than with a corresponding increase of the initial vibrational excitation. This means that the amount of energy disposed in translation is more efficient in promoting reactivity than that disposed in vibration. This agrees with what was previously found for the LEPS surface. As a matter of fact, at low temperature, the system is scarcely reactive irrespective of the vibrational excitation of the reactants, while, even at low vibrational energy, the reaction efficiency is high when T is high.

Among the LAGROBO surfaces, the L0 PES is the least reactive at all temperatures and initial vibrational levels. L1 state specific reactive rates are larger than those of L0 at all v values. The difference, however, decreases as the temperature increases. This implies that the displacement of the transition state geometry to tighter angles, though decreasing with the system energy, makes it more efficient to transfer collision energy into effective motion along the reaction path. Our results indicate also that similar effects are induced by the modification of bond lengths at the transition state. As far as L1 and L2 are concerned, the former PES leads to larger $k_v(T)$ values than the latter. The difference increases with v due to the fact that the incoming atom is able to come closer to the target diatom in the transition state region. The effect of decreasing the height of the barrier is also evidenced by our results. The value of

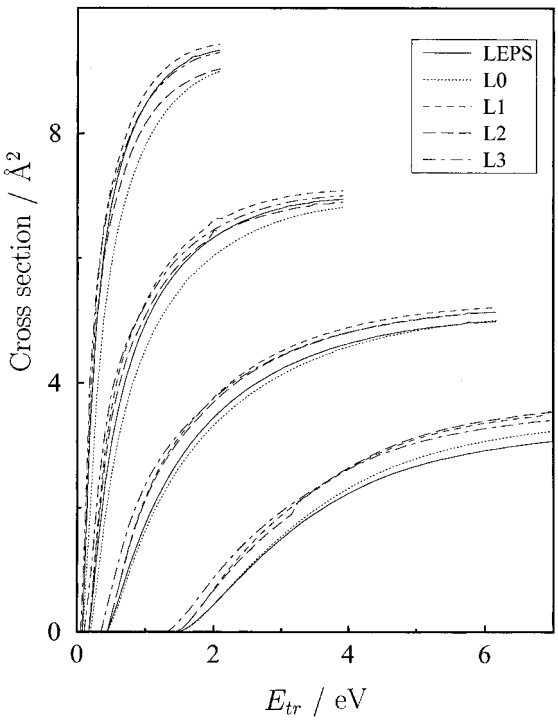

Figure 1. RIOS cross sections $\sigma_v(E_{tr})$ for the different PESs at $v = 0$ (lower set), $v = 10$ (central lower set), $v = 20$ (central upper set), and $v = 30$ (upper set) plotted as a function of translational energy.

$k_v(T)$, in fact, increases on going from L1 to L3. The difference is more than appreciable at small v values, while it becomes less appreciable at larger v values especially as the temperature increases. The v value at which L1 and L3 reactive rates become comparable lowers as T increases. This agrees again with the fact that the role of the transition state height becomes less important as energy increases.

The dependence on v of the state specific reactive rates calculated on the LEPS PES differs appreciably from that calculated on LAGROBO surfaces. On the one hand, at low vibrational energy state specific reactive rates calculated on the LEPS are, in general, smaller than those calculated on L1, L2, and L3 surfaces (which have a bent transition state). On the other hand, as v increases, reactive rates calculated on the LEPS increase more rapidly than those calculated on LAGROBO surfaces. As far as state specific rates calculated on L0 is concerned, they coincide with those calculated on the LEPS at low vibrational energy. At larger v values, however, L0 reactivity is smaller than that calculated on the LEPS, implying that the features of the LAGROBO surfaces experienced at high energy favor reactivity less than those experienced on the LEPS.

A less averaged quantity, allowing a better understanding of the propensity to reaction of the different PESs, is the state specific cross section $\sigma_v(E_{tr})$. In our case this quantity was explicitly calculated only using the quantum RIOS method. The values of $\sigma_v(E_{tr})$ calculated at $v = 0$, 10, 20, and 30 are plotted in Figure 1. State specific cross sections always lead to a plateau after steeply increasing at threshold, as typical of barrier-controlled reactions. Both the slope of the increasing part of the plot and the height of the associated plateau increase as v increases. A first difference worth pointing out is concerned with translational energy thresholds. For L3 (the PES having the lowest transition state) the threshold energy is lower than that for LEPS, L0, L1, and L2 (they all have the same threshold and transition state height). At energy values close to threshold, L0 is less reactive than the remaining LAGROBO surfaces. This difference increases with v and decreases with collision energy.

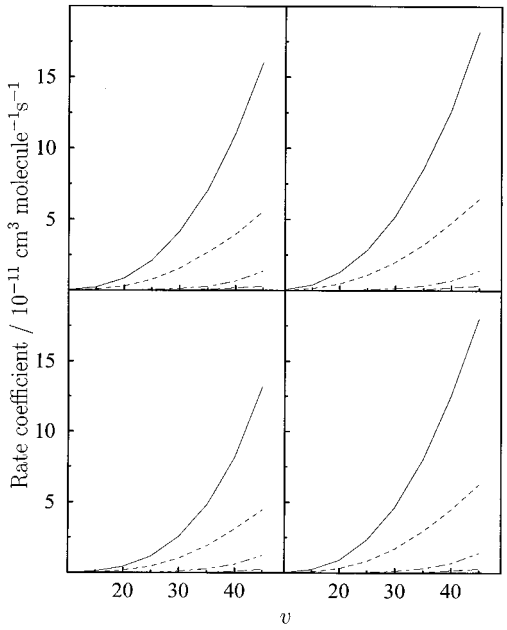

Figure 2. QCT deexcitation and excitation rate coefficients calculated at $T = 1000$ K plotted as a function of v for L0 (lower lhs panel), for L1 (lower rhs panel), for L2 (upper lhs panel), and for L3 (upper rhs panel) surfaces: reactive deexcitation (solid line), nonreactive deexcitation (dashed line), reactive excitation (dashed dotted line), and nonreactive deexcitation (long dashed line).

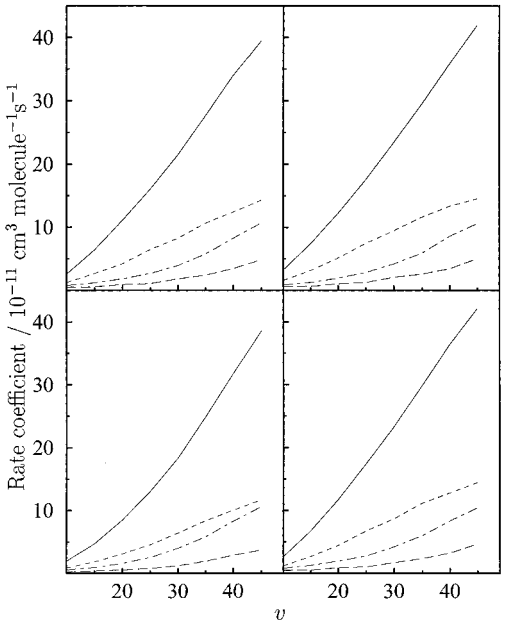

Figure 3. QCT deexcitation and excitation rate coefficients calculated at $T = 4000$ K plotted as a function of v for L0 (lower lhs panel), for L1 (lower rhs panel), for L2 (upper lhs panel), and for L3 (upper rhs panel) surfaces: reactive deexcitation (solid line), nonreactive deexcitation (dashed line), reactive excitation (dashed dotted line), and nonreactive deexcitation (long dashed line).

L1 and L2 though having different bond lengths at the transition state (yet, the energy is the same) led to an identical value for the state specific cross section near the threshold. The L1 $\sigma_v(E_{tr})$, however, becomes larger at larger energies except that at $v = 0$. L3 is the surface leading to the largest value of the cross section and to the faster reach of the plateau. At $v = 0$, the LEPS state specific reactive cross section is the same as that of L0 about near threshold and becomes smaller at larger energies. Its dependence on v, however, is stronger than for L0 and makes it larger than the state specific rates calculated on L2 and L3. The difference tends to vanish once reaching the plateau. It is worth pointing out, however, that only the lowest vibrational states and translational energies contribute significantly to the value of the 3400 K thermal rate.

3.4. State to State Reactivity. The most detailed analysis of the properties of a reactive process can be performed using state to state cross sections ($\sigma_{vv'}(E_{tr})$) and rate coefficients ($k_{vv'}(T)$). These quantities are also important for practical use since they allow a realistic modeling of cold plasmas (as the air shell surrounding reentering spacecraft[2]). Sometimes, partial summations of state to state rate coefficients are also used. In particular, we discuss here the vibrational deexcitation $k_v^d(T) = \sum_{v'<v} k_{vv'}(T)$ and excitation $k_v^e(T) = \sum_{v'>v} k_{vv'}(T)$ rates.

As an example of the behavior of these quantities for the different LAGROBO surfaces, we plot in Figures 2 and 3 the value of the deexcitation and excitation (reactive and nonreactive) rates calculated using QCT methods as a function of the initial vibrational number. The calculations have been performed for T varying from 500 to 4000 K (we omit here the plots for $T = 500$ and 2000 since they do not differ from the ones shown here). Both figures show that the dominant process is always vibrational deexcitation (reactive and nonreactive, with the former being the largest one). Excitation processes are unimportant at low temperature. However, they increase appreciably with the temperature to become larger than vibrationally adiabatic ones. Essentially, the behavior of deexcitation and excitation rate coefficients calculated on the LAGROBO surfaces is similar to that calculated on the LEPS. The relative

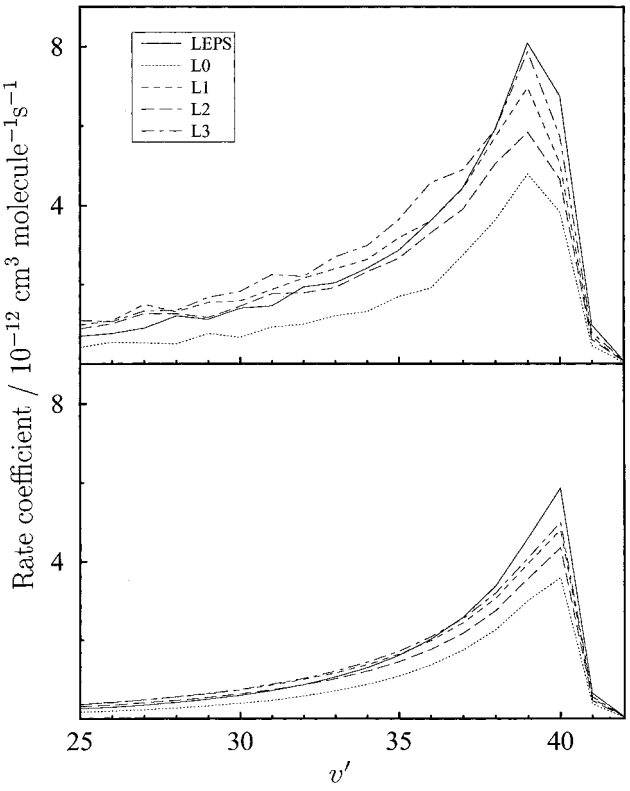

Figure 4. QCT (upper panel) and RIOS (lower panel) state to state rate coefficients calculated at $v = 40$ and $T = 500$ K plotted as a function of v'.

variation of the rate coefficients for reactive deexcitation on the different potential energy surfaces shows strong similarities with what was found for state specific rates $k_v(T)$. The nonreactive vibrational deexcitation always behaves differently from reactive deexcitation: the largest nonreactive vibrational deexcitation takes place on L3, L1, and L2 (in this order), while the smaller ones take place on the LEPS and L0. This trend weakens as v increases, and the difference between the two sets

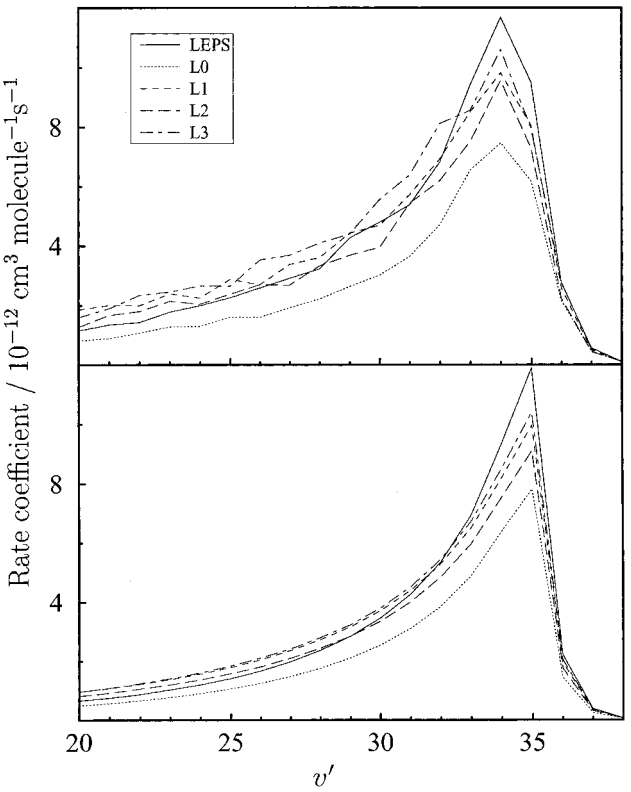

Figure 5. QCT (upper panel) and RIOS (lower panel) state to state rate coefficients calculated at $v = 35$ and $T = 1000$ K plotted as a function of v'.

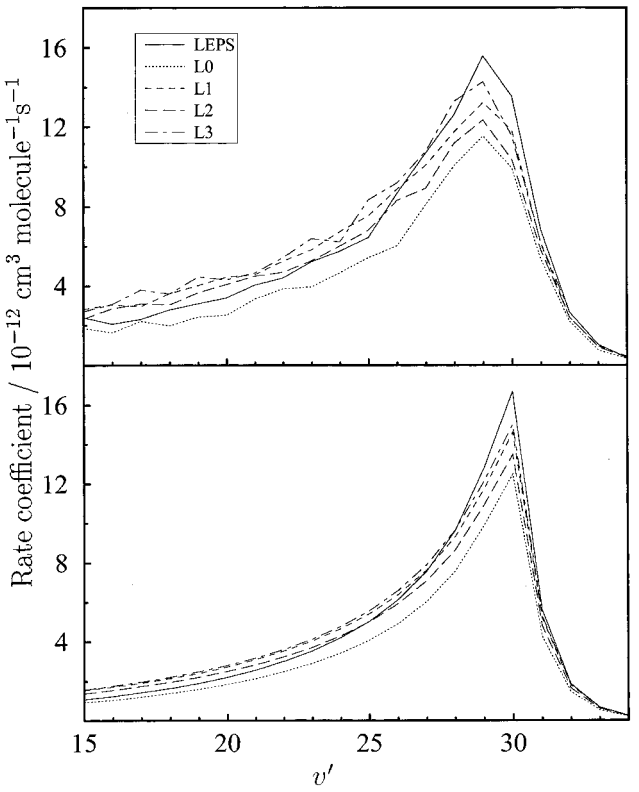

Figure 6. QCT (upper panel) and RIOS (lower panel) state to state rate coefficients calculated at $v = 30$ and $T = 2000$ K plotted as a function of v'.

of results increases with the temperature. Reactive and nonreactive excitation processes are less efficient. Therefore, also their variations are less noticeable.

QCT state to state rate coefficients $k_{vv'}(T)$ calculated at various temperatures and vibrational states on the different LAGROBO surfaces (see upper panels of Figures 4−7) have the same qualitative features. Related product vibrational distributions have approximately the same shape with a peak located at $v' = v - 1$ as for LEPS results. The most significant difference is concerned with the absolute value of the maximum that, as for state specific quantities, is lower for L0 than for other LAGROBO surfaces. This means that single quantum jumps are the basic component of any vibrational relaxation process, although for LAGROBO surfaces having a bent transition state there is a higher propensity to give multiquantum jumps.

Essentially the same behavior was observed for RIOS results (see lower panels of Figures 4−7). However, between QCT and RIOS results there is a difference very important to single out. RIOS results, in fact, have on all surfaces a maximum at $v' = v$. This means that, contrary to QCT results, RIOS vibrational deexcitation (as a single event) is not the dominant one. At the same time, multiquantum deexcitations are less likely to occur. This leads to an overall poorer effectiveness in vibrational deexcitation efficiency, although the overall effect is still quite large. More extended tables reporting in detail the values of state to state rate coefficients for all the surfaces using both QCT and RIOS methods are given as Supporting Information.[18]

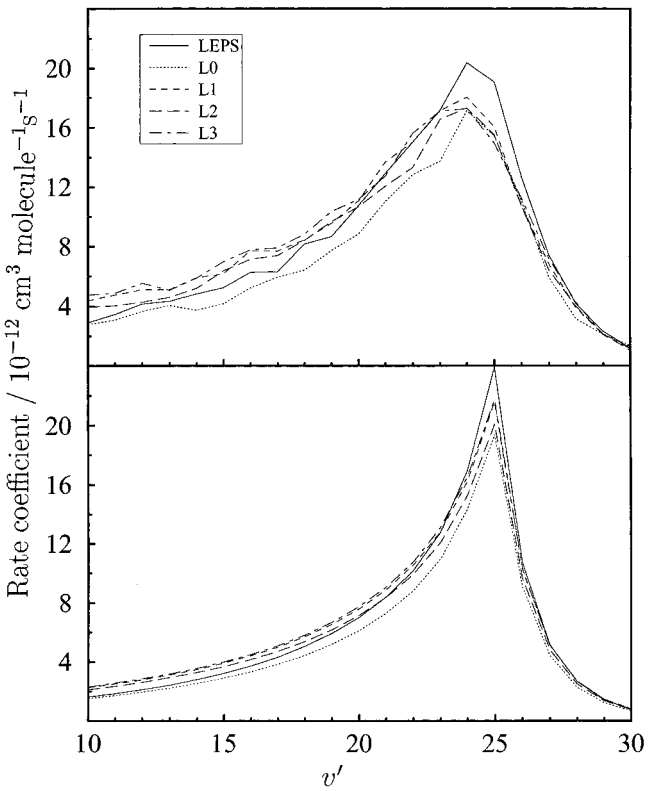

Figure 7. QCT (upper panel) and RIOS (lower panel) state to state rate coefficients calculated at $v = 25$ and $T = 4000$ K plotted as a function of v'.

4. Conclusions

Our investigation of the effect of varying the geometry of the transition state on the state specific and state to state reactive properties of the N + N_2 system has led to the following conclusions.

Quasiclassical and infinite order sudden cross sections calculated on different LAGROBO sufaces indicate that a displacement of the transition state from large to tight collision angles makes it more efficient to transfer collision energy into

effective motion along the reaction path. Analogous results can be obtained also by modifying the length of the transition state bonds.

Quasiclassical and infinite order sudden state to state rate coefficients $k_{v v'}(T)$ calculated on different LAGROBO sufaces at various temperatures and vibrational states have the same qualitative features. Related product vibrational distributions have approximately the same shape with a peak located at $v' = v - 1$, as for LEPS results. The most significant difference is concerned with the absolute value of the maximum that, as for state specific quantities, is lower for L0 than for other LAGROBO surfaces. This means that single quantum jumps are the basic component of any vibrational relaxation process, although LAGROBO surfaces having a bent transition state have a higher propensity to give multiquantum jumps.

Acknowledgment. The authors wish to thank the Italian Space Agency (ASI), the Progetti Finalizzati of CNR (Italy), and the Spanish DGICYT (Grant PB95−0930) for financial support.

References and Notes

(1) Armenise, I.; Capitelli, M.; Garcia, E.; Gorse, C.; Laganà, A.; Longo, S. *Chem. Phys. Lett.* **1992**, *200*, 597.

(2) Armenise, I.; Capitelli, M.; Celiberto, R.; Colonna, G.; Gorse, C.; Laganà, A. *Chem. Phys. Lett.* **1994**, *227*, 157.

(3) Laganà, A.; Riganelli, A.; Ochoa de Aspuru, G.; Garcia, E.; Martinez, T. In *Molecular physics and hypersonic flows*; Capitelli, M., Ed.; Kluwer: Dordrecht, 1996; p 35.

(4) Laganà, A.; Garcia, E.; Ciccarelli, L. *J. Phys. Chem.* **1987**, *91*, 312.

(5) Garcia, E.; Laganà, A. *J. Phys. Chem.* **1994**, *98*, 502.

(6) Petrongolo, C. *J. Mol. Struct.* **1988**, *175*, 215.

(7) Petrongolo, C. *J. Mol. Struct. (THEOCHEM)* **1989**, *202*, 135.

(8) Laganà, A.; Garcia, E. *J. Chem. Phys.* **1995**, *103*, 5410.

(9) Laganà, A.; Ochoa de Aspuru, G.; Garcia, E. *J. Phys. Chem.* **1995**, *99*, 17139.

(10) Laganà, A. *J. Chem. Phys.* **1991**, *95*, 2216.

(11) Laganà, A.; Ferraro, G.; Garcia, E.; Gervasi, O.; Ottavi, A. *Chem. Phys.* **1992**, *168*, 341.

(12) Truhlar, D. G.; Muckerman, J. T. in *Atom molecule collision theory: a guide for the experimentalist*; Bernstein, R. B., Ed.; Plenum: New York, 1979; Chap. 16. Bunker, D. L. *Methods Comput. Phys.* **1971**, *10*, 287. Raff, M. L.; Thompson, D. L. In *Theory of chemical reaction dynamics*; Baer, M., Ed.; CRC Press: Boca Raton, 1985; Vol. III, p 1.

(13) Jellinek, J.; Kouri, D. J. In *Theory of chemical reaction dynamics*, Baer, M., Ed.; CRC Press: Boca Raton, 1985; Vol. II, p 1. Laganà, A.; Garcia, E.; Gervasi, O. *J. Chem. Phys.* **1988**, *89*, 7238.

(14) Huber, K. P.; Herzberg, G. *Molecular spectra and molecular structure. IV Constants of diatomic molecules*; Van Nostrand: Amsterdam, 1979.

(15) Laganà, A.; Ochoa de Aspuru, G.; Garcia, E. Technical Report AIAA 94--1986, 1994.

(16) Back, R. A.; Mui, J. Y. P. *J. Phys. Chem.* **1962**, *66*, 1362.

(17) Bar-Nun, A.; Lifshitz, A. *J. Chem. Phys.* **1967**, *47*, 2878.

(18) Laganà, A.; Garcia, E. *Quasiclassical rate coefficients for the H + H_2 reaction*; Università di Perugia, Centro Stampa, 1996. Laganà, A.; Ochoa de Aspuru, G.; Garcia, E. *Quasiclassical and quantum rate coefficients for the N + N_2 reaction*; Università di Perugia: Centro Stampa, 1996.

(19) Gorse, C.; Capitelli, M.; Bacal, M.; Bretagne, J.; Laganà, A. *Chem. Phys.* **1987**, *117*, 177. Gorse, G.; Celiberto, R.; Cacciatore, M.; Laganà, A.; Capitelli, M. *Chem. Phys.* **1992**, *161*, 211.